

Computational and Experimental Analyses Reveal the Essential Roles of Interdomain Linkers in the Biological Function of Chemotaxis Histidine Kinase CheA

Xiqing Wang,[†] Chun Wu,[†] Anh Vu, Joan-Emma Shea,* and Frederick W. Dahlquist*

Department of Chemistry and Biochemistry, University of California Santa Barbara, Santa Barbara, California 93106, United States

Supporting Information

ABSTRACT: A two-component signal transduction pathway underlies the phenomenon of bacterial chemotaxis that allows bacteria to modulate their swimming behavior in response to environmental stimuli. The dimeric five-domain histidine kinase, CheA, plays a central role in the pathway, converting sensory signals to a chemical signal via trans-autophosphorylation between the P1 and P4 domains. This autophosphorylation is regulated via the networked interactions among the P5 domain of CheA, CheW, and chemoreceptors. Despite a wealth of structural information about these components and their interactions, the key question of how the kinase activity of the catalytic P4 domain is regulated by the signal received from the regulatory P5 domain remains poorly understood. We performed replica exchange molecular dynamics simulations on the CheA kinase core and found that while individual domains maintained their structural fold, these domains exhibited a variety of interdomain orientations due to two interdomain linkers. A partially populated conformation that adopts an interdomain arrangement is suitable for building a functional ternary complex. An allosteric network derived from this structural model implies critical roles for two linkers in CheA's activity. The biochemical and biological functions of these linkers were assigned via a series of biochemical and genetic assays that show the P4–P5 linker controls the activation of CheA and the P3–P4 linker controls both the basal autophosphorylation activity and the activation of CheA. These results reveal the functional dependence between the two linkers and the essential role of the linkers in passing signal information from one domain to another.

Two-component signal transduction systems, involving a histidine kinase (HK) and a response regulator (RR), are important mechanisms by which bacteria and fungi sense, respond, and adapt to a changing environment.^{1,2} Absent in mammals, HKs have been targets for the development of novel antimicrobial drugs.^{3–5}

In bacterial chemotaxis, an HK–RR pair enables the biased movement of a bacterium toward favorable and away from unfavorable conditions.⁶ Specifically, the binding of ligands to transmembrane chemoreceptors (called methyl-accepting chemotaxis proteins/MCPs) in the cell's inner membrane leads to a response at the flagellar motor through an HK–RR mechanism. The HK CheA plays a central role in this signaling

pathway: converting the extracellular signal, transduced by MCPs, to a flux of phosphoryl groups to the RR, CheY, in the cytosol at the expense of ATP. Phosphorylated CheY interacts directly with the flagellar motor, enhancing flagellar reversal and cell tumbling. The kinase activity of CheA requires a coupling protein, CheW that serves as an adapter, coupling MCPs, and CheA.⁷ The kinase activity of CheA, in complex with CheW and receptors, is highly regulated, depending on both receptor ligand occupancy and methylation level.

CheA consists of five domains linked by four flexible linkers: the histidine-containing phosphotransfer domain (P1), the CheY binding domain (P2), the dimerization domain (P3), the ATP-binding/catalytic domain (P4), and the regulatory domain (P5) (Figure S1). Dimerization of CheA is required for its activity.⁸ Trans-autophosphorylation occurs by the P4 domain of one subunit catalyzing phosphotransfer from ATP to a conserved histidine residue in the P1 domain of the other subunit.⁹ Free CheA undergoes basal autophosphorylation (P4→P1) at a slow rate. However, in complex with CheW and MCPs via its P5 domain, CheA's kinase activity can change dramatically: the apo or repellent-bound receptor can activate autophosphorylation several hundred fold compared to the attractant-bound state.^{10,11} The P3, P4, and P5 domains together form a kinase core that phosphorylates an isolated P1 domain *in trans* and supports chemotaxis *in vivo*.¹² Thus, the minimum protein complex needed for stimulus-response coupling consists of MCPs, CheW, dimeric P3P4P5, and the P1 domain.

The structure of the dimeric P3P4P5 kinase core of CheA has been determined,¹³ and its interactions with CheW and chemoreceptors have been characterized by various methods.^{14–18} The gross architecture of the ternary complex has been examined by EM^{18–20} and crystallography¹⁸ and has been proposed with various constraints.^{17,21} A common feature of the architecture is that both the putative stimulus-input sites on the P5 domain and the dimerization P3 domain are more than 45 Å away from the responsive catalytic site of the P4 domain. The lack of direct physical contacts among these domains raises a number of important questions: (1) How does the P3 domain affect the kinase activity of the P4 domain? While retaining a stable fold and ATP binding, the isolated P4 domain is at least a thousand times less active than the P3P4 construct.²² It seems that some subtle conformational changes in the P4 domain

Received: June 11, 2012

induced by the P3 domain via the P3–P4 linker are required for the phosphorylation ability of the P4 domain. (2) How does the P5 domain regulate the phosphotransfer from the P4 domain to the P1 domain? Only the P5 domain is responsible for interacting with CheW and receptors to regulate phosphotransfer between the P4 and P1 domains. This suggests that the P4–P5 linker may play an important role in this communication between the P5 and P4 domains.

Growing evidence points to significant interdomain dynamics. The crystal structures of the P3P4P5 dimer¹³ and P4P5–CheW complex,¹⁴ as well as a recent low-resolution crystal structure of P4P5–CheW–receptor fragment (Tm14s) ternary complex,¹⁸ show different domain arrangements. Moreover, disulfide bonds can be formed between two apparently distal residues in the kinase core, which suggests that the motions are in fact much larger than the crystal structures suggest.²³

Here, we combined all-atom replica-exchange molecular dynamics (REMD) simulations and a series of biochemical and genetic assays of point mutants at the P3–P4 and P4–P5 linkers to probe the critical role of the linkers in modulating interdomain dynamics associated with both basal autophosphorylation and activation of histidine kinase. Our simulation results show that the individual domains, while exhibiting some structural fluctuations, maintain the overall structural fold of CheA. The domains are seen to exhibit a variety of orientations relative to each other due to the dynamics of the linkers. Based on these simulations we generated mutations in the P3–P4 or P4–P5 linker using *E. coli* CheA. These show that these linkers play critical but different roles. Whereas single-point mutations in the P3–P4 linkers decreased both the basal autophosphorylation and the activation of CheA, single-point mutations at the P4–P5 linker retained the basal autophosphorylation activity but greatly impaired the activation of CheA. The combined results provide insight into how the signal is transduced across a long distance in this multiple domain protein.

Details of the simulations are given in the Supporting Information (SI). As shown from the $C\alpha$ root-mean-square deviations plotted in Figure S2, the interdomain (rather than intradomain) structural fluctuations of the CheA monomer dominate the overall structural fluctuation of the system. We characterize the intradomain dynamics by calculating the root-mean-square fluctuations (RMSF) of each domain. The dynamic fluctuations within the three individual domains are consistent with previous studies on these domains. The computational results and a detailed description of the intradomain dynamics are presented in Figure S3.

Our simulation results show that motions in the linkers give rise to a large amount of interdomain arrangement among the three domains. We found that, although the two linkers that connect the three domains were extremely dynamic, the joint among the three domains did not move significantly (Figure S4). Therefore we defined the center of the joint (defined as the center of mass of the two linkers; see Figure S4) as the origin of the protein, allowing us to characterize the hinge motion between pairs of domains. The angle distributions using the three vectors pointing from the origin to the center of the three domains are shown in Figure 1. The multipeak feature of the distribution indicates that a free CheA adopts multiple conformational states. Previous structural studies on the binary (CheA–CheW,¹⁴ CheW–receptor,^{18,24} and CheA–receptor^{15,18}) interactions in the ternary complex suggested that, based on the domain orientation in the crystal structure of the

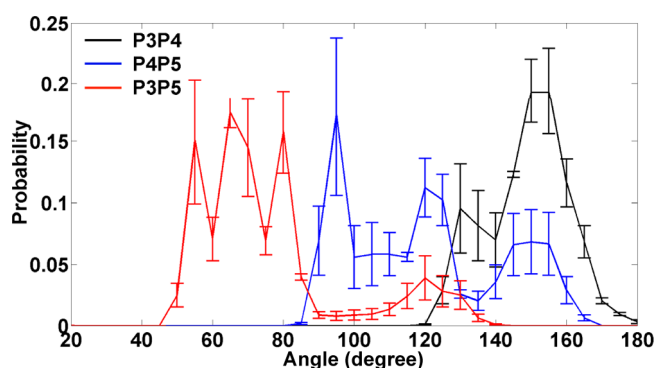


Figure 1. Angles between pairs of the P3, P4, and P5 domains.

P3P4P5 dimer (P4P5 angle $\sim 100^\circ$, P3P4 angle $\sim 125^\circ$, and P3P5 angle $\sim 65^\circ$), the binding sites involved in the formation of the ternary complex conflict with the transmembrane nature of chemoreceptors (Figure S5a).^{15,17,21} To determine if the distribution includes the conformation required for formation of the signaling complex with CheW and the chemoreceptor, we first identified structural families by a clustering analysis (SI methods). The five most populated structural families are shown in Figure S6. We compared angles calculated for each of these computational families to those obtained from available crystal structures. Table 1 lists the angles between domains of

Table 1. Angles between Domains of CheA Kinase Core in Different Structures and Conformations^a

structure	angle between two domains		
	P3P4	P4P5	P3P5
P3P4P5 conformation A	126°	103°	67°
P3P4P5 conformation B	127°	100°	66°
P4P5–CheW conformation A	–	124°	–
P4P5–CheW conformation B	–	99°	–
P4P5–CheW–Tm14s	–	120°	–
Cluster 3	150 \pm 5°	119 \pm 3°	79 \pm 2°

^aThe crystal structures of the P3P4P5 dimer¹³ and P4P5–CheW complex¹⁴ show two conformations denoted as A and B. The crystal structures of the P4P5–CheW complex¹⁴ and P4P5–CheW–Tm14s ternary complex¹⁸ miss the P3P4 and P3P5 angles.

CheA for three crystal structures, the P3P4P5 dimer,¹³ P4P5–CheW complex,¹⁴ and P4P5–CheW–Tm14s ternary complex.¹⁸ The P4P5 angle shows roughly two values ($\sim 100^\circ$ and $\sim 120^\circ$) in the crystal structures. Cluster 3 from our simulations (Figure S6) is consistent with the low-resolution P4P5–CheW–Tm14s ternary complex,¹⁸ with an angle of $\sim 120^\circ$ between the P4 and P5 domains. The $\sim 120^\circ$ P4P5 angle, together with the other two angles (P3P4 angle $\sim 150^\circ$ and P3P5 angle $\sim 80^\circ$), fully exposes the P4 domain to the solvent and aligns receptor binding sites of CheW and the P5 domain to the receptor tip region, thus reconciling the structural incompatibility between CheA and its interactions with CheW and receptors (Figure 2, left and Figure S5b and c). A structural model of the signaling complex is shown in Figure 2, where the position of the P3 helices is derived directly from the MD data and was missing in the crystal structure.¹⁸ Moreover, the domain organization changes in cluster 3 are the same as those in the EM reconstruction of the *in vivo* complex as compared to the crystal structure of the kinase alone.^{18,20} This suggests that the interdomain dynamics of free CheA offer an ensemble of

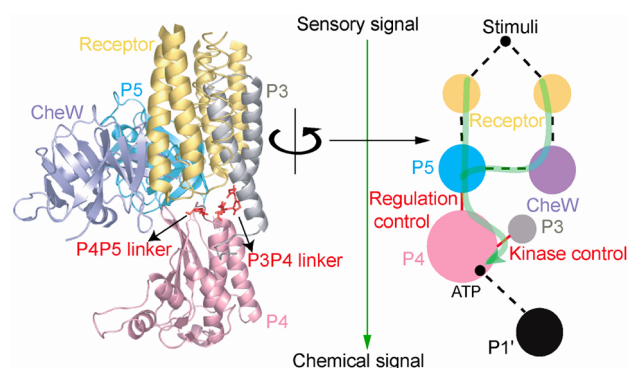


Figure 2. Structural model of signaling complex (left; see Figure S5d for details) and a network scheme²⁶ of chemotaxis signal transduction pathway (right, dash line: protein–protein interaction, solid line: interdomain linker). The structural model is built with monomeric CheA kinase core in cluster 3 conformation, CheW, and two receptor dimers. These proteins are assembled based on the results from previous structural studies on the binary protein–protein interactions among them, including the crystal structure of the P4P5–CheW complex¹⁴ and the NMR data on CheW–receptor²⁴ and P4P5–receptor¹⁵ interactions (see Figure S5c for these contacts). The antiparallel orientation between the P3 domain and the receptor is required to achieve the assembly (see Figure S5), which is consistent with previous ESR data.²¹ The construction of this model is independent of, but consistent with, the crystal structure of the P4P5–CheW–TM14s complex and EM-reconstructed native signaling complex.^{18,20}

conformational states and that the association of CheA with the transmembrane receptor results from its interactions with MCPs and CheW that select and stabilize the pre-existing conformations of CheA (i.e., those seen in cluster 3, ~23% of the total ensemble, Figure S6) for forming the signaling complex, as recently proposed by Nussinov et al.²⁵ Functionally, this CheA–CheW–receptor ternary complex is a regulating platform where the receptor affects the conformation of the kinase core by interacting with CheW and the P5 domain. While CheW and the P5 domain of CheA carry the structural determinants for receptor binding, the two interdomain linkers may be required to mediate proper conformational changes in the kinase core, transmitting the signal from the level of P5–CheW–receptor interaction to the catalytic P4 domain.

We perturbed the two interdomain linkers in *E. coli* CheA by mutagenesis and tested the resulting mutants in a series of assays. Previous structural studies show that the signaling complex is assembled on the interaction network among chemoreceptors, CheW, and the P5 domain of CheA and that the linkers are not involved in the interactions of CheA with CheW and receptor.^{14,18} Consistent with these observations, the mutation of the linker residues results in CheA variants that were still able to form stable ternary complexes with CheW and the cytoplasmic domain of *E. coli* chemoreceptor Tsr. (Figure S7). However, the mutations affected the function of CheA in different ways. Single amino acid replacement (L507A, T508A, and L509A; see Figure S8) at the P4–P5 linker retained basal autophosphorylation activity, showing similar autophosphorylation rates to wild-type CheA or the CheA– Δ P5 construct (Figure 3a) but greatly impaired *in vitro* kinase activation by Tsr (Figure 3b) and failed to support chemotaxis (Figure 3c) (SI methods). These results indicate that, while these mutants were still capable of performing kinase autophosphorylation and

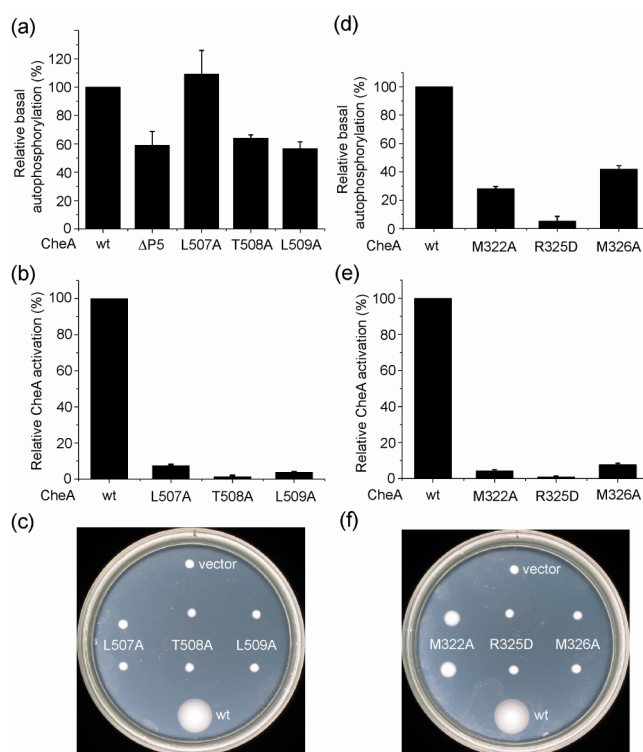


Figure 3. Mutational analysis of the linker residues. (a, d) ATPase assays (s.d., $n = 3$) for the basal autophosphorylation activities; (b, e) *in vitro* CheA activation assays (s.d., $n = 3$) for the activation abilities; and (c, f) *in vivo* swarm assays (duplicate for the mutants) for the chemotactic abilities of *E. coli* CheA variants. (a–c) The P4–P5 linker; (d–f) the P3–P4 linker.

forming a ternary complex with CheW and the receptor, the input signal transmitted from the receptor to the P5 domain is not able to successfully regulate the P4 domain. The drastic change in CheA activation by these point mutations indicates that this linker is essential to transform CheA to its activated state. In contrast, the insensitivity of the basal autophosphorylation to the changes in the linker suggests that the basal autophosphorylation activity arises from another much less active state of free CheA. On the other hand, mutation of the P3–P4 linker residues (M322A, R325D, and M326A; see Figure S9) decreased the basal autophosphorylation of CheA (Figure 3d) and abolished kinase activation by Tsr (Figure 3e). In contrast to an attractant ring shown by the wild-type CheA expressing strain, all the mutants failed to show a swarm ring in the swarm assays (Figure 3f). Such dramatic changes caused by single amino acid replacement in this linker indicate that the dynamics between the P3 and P4 domains may govern both the basal autophosphorylation and activation of CheA. The P4 domain is flanked between the P3 and P5 domains by the P3–P4 and P4–P5 linkers. These results show that, even if the P4–P5 linker is intact in these P3–P4 linker mutants, the chemoreceptor fails to activate CheA, suggesting that dynamics between the P4 and P5 domains requires further support by that between the P3 and P4 domains to achieve kinase activation in the P4 domain.

The interdomain dynamics of the CheA kinase core probed by REMD simulation and the assignment of the function of each interdomain linker by mutational studies indicate that the activation of CheA results from two sequential dynamic controls: regulation control mediated by the P4–P5 linker

and kinase activity control achieved by the P3–P4 linker. These results also provide insight into the mechanism of how the signal is transduced across a long distance to achieve CheA regulation (Figure 2). Chemotactic signals are detected by the periplasmic domains of receptors and further transduced into the cytosol where the cytoplasmic domains of receptors form complexes with CheA and CheW by selecting the partially populated state (cluster 3) from the structural ensemble of CheA. The interactions of the cytoplasmic domain of the receptor with CheW and the P5 domain of CheA enable the signal to reach the level of CheW and the P5 domain, where CheW and the P5 domain also bind together. Successful regulation of CheA activity requires a further signal transmission from the P5–CheW level to the P4 domain assisted by the P4–P5 linker and the downstream P3–P4 linker that are required to maintain the proper domain orientation in CheA kinase core. Our results suggest that changes in domain positioning could account for the differences between inactive and activated states of CheA. In addition, since the interdomain dynamics between the P3 and P4 domains is also crucial to the basal autophosphorylation, it now becomes clear why the isolated P4 domain shows much less enzymatic activity than the P3P4 construct.

The majority of prokaryote and eukaryote proteins have multiple domains, typically connected by flexible linkers.²⁷ This study shows that, beyond simply bringing two domains closer together, thereby increasing the effective concentration of reactants and shortening the time scales of signaling steps,²⁸ some interdomain linkers exert a more complex control by dynamically mediating communication among domains. Targeting these functional interdomain linkers may emerge as an effective strategy for drug design.

■ ASSOCIATED CONTENT

Supporting Information

Description of all experimental procedures and supporting figures. This material is available free of charge via the Internet at <http://pubs.acs.org>.

■ AUTHOR INFORMATION

Corresponding Author

dahlquist@chem.ucsb.edu; shea@chem.ucsb.edu

Author Contributions

[†]X.W. and C.W. contributed equally to this work.

Notes

The authors declare no competing financial interest.

■ ACKNOWLEDGMENTS

We thank the members of the Parkinson laboratory (University of Utah) for providing strains and advice. This work was supported by NIH Grant GM59544 (to F.W.D.) and NSF Grant MCB-1158577 (to J.-E.S.). Simulations were performed using the XSEDE resources (Grant TG-MCA05S027) supported by the NSF (Grant OCI-1053575).

■ REFERENCES

- (1) Gao, R.; Mack, T. T.; Stock, A. M. *Trends Biochem. Sci.* **2007**, *32*, 225.
- (2) Parkinson, J. S.; Kofoid, E. C. *Annu. Rev. Genet.* **1992**, *26*, 71.
- (3) Watanabe, T.; Okada, A.; Gotoh, Y.; Utsumi, R. *Adv. Exp. Med. Biol.* **2008**, *631*, 229.
- (4) Barrett, J. F.; Hoch, J. A. *Antimicrob. Agents Chemother.* **1998**, *42*, 1529.
- (5) Kurosu, M.; Begari, E. *Drug Dev. Res.* **2010**, *71*, 168.
- (6) Wadhams, G. H.; Armitage, J. P. *Nat. Rev. Mol. Cell Biol.* **2004**, *5*, 1024.
- (7) Gegner, J. A.; Graham, D. R.; Roth, A. F.; Dahlquist, F. W. *Cell* **1992**, *70*, 975.
- (8) Surette, M. G.; Levit, M.; Liu, Y.; Lukat, G.; Ninfa, E. G.; Ninfa, A.; Stock, J. B. *J. Biol. Chem.* **1996**, *271*, 939.
- (9) Swanson, R. V.; Bourret, R. B.; Simon, M. I. *Mol. Microbiol.* **1993**, *8*, 435.
- (10) Borkovich, K. A.; Kaplan, N.; Hess, J. F.; Simon, M. I. *Proc. Natl. Acad. Sci. U.S.A.* **1989**, *86*, 1208.
- (11) Bourret, R. B.; Davagnino, J.; Simon, M. I. *J. Bacteriol.* **1993**, *175*, 2097.
- (12) Garzón, A.; Parkinson, J. S. *J. Bacteriol.* **1996**, *178*, 6752.
- (13) Bilwes, A. M.; Alex, L. A.; Crane, B. R.; Simon, M. I. *Cell* **1999**, *96*, 131.
- (14) Park, S.; Borbat, P. P.; Gonzalez-Bonet, G.; Bhatnagar, J.; Pollard, A. M.; Freed, J. H.; Bilwes, A. M.; Crane, B. R. *Nat. Struct. Mol. Biol.* **2006**, *13*, 400.
- (15) Wang, X.; Vu, A.; Lee, K.; Dahlquist, F. W. *J. Mol. Biol.* **2012**, *422*, 282.
- (16) Zhao, J.; Parkinson, J. S. *J. Bacteriol.* **2006**, *188*, 4321.
- (17) Miller, A. S.; Kohout, S. C.; Gilman, K. A.; Falke, J. J. *Biochemistry* **2003**, *42*, 2952.
- (18) Briegel, A.; Li, X.; Bilwes, A. M.; Hughes, K. T.; Jensen, G. J.; Crane, B. R. *Proc. Natl. Acad. Sci. U.S.A.* **2012**, *109*, 3766.
- (19) Francis, N. R.; Wolanin, P. M.; Stock, J. B.; Derosier, D. J.; Thomas, D. R. *Proc. Natl. Acad. Sci. U.S.A.* **2004**, *101*, 17480.
- (20) Liu, J.; Hu, B.; Morado, D. R.; Jani, S.; Manson, M. D.; Margolin, W. *Proc. Natl. Acad. Sci. U.S.A.* **2012**, *109*, E1481.
- (21) Bhatnagar, J.; Borbat, P. P.; Pollard, A. M.; Bilwes, A. M.; Freed, J. H.; Crane, B. R. *Biochemistry* **2010**, *49*, 3824.
- (22) Bilwes, A. M.; Quezada, C. M.; Croal, L. R.; Crane, B. R.; Simon, M. I. *Nat. Struct. Biol.* **2001**, *8*, 353.
- (23) Gloor, S. L.; Falke, J. J. *Biochemistry* **2009**, *48*, 3631.
- (24) Vu, A.; Wang, X.; Zhou, H.; Dahlquist, F. W. *J. Mol. Biol.* **2012**, *415*, 759.
- (25) Ma, B.; Tsai, C.; Haliloglu, T.; Nussinov, R. *Structure* **2011**, *19*, 907.
- (26) Nussinov, R.; Tsai, C. J.; Csermley, P. *Trends Pharmacol. Sci.* **2011**, *32*, 686.
- (27) Apic, G.; Huber, W.; Teichmann, S. A. *J. Struct. Funct. Genomics* **2003**, *4*, 67.
- (28) Marcotte, E. M.; Pellegrini, M.; Ng, H. L.; Rice, D. W.; Yeates, T. O.; Eisenberg, D. *Science* **1999**, *285*, 751.